NASA TECHNICAL NOTE

NASA TN D-2259

NASA TN D-2259

AN INSTABILITY EFFECT ON TWO-PHASE HEAT TRANSFER FOR SUBCOOLED WATER FLOWING UNDER CONDITIONS OF ZERO GRAVITY

by S. Stephen Papell

Lewis Research Center

Cleveland, Ohio

NATIONAL AERONAUTICS AND SPACE ADMINISTRATION • WASHINGTON, D. C. • NOVEMBER 1964

AN INSTABILITY EFFECT ON TWO-PHASE HEAT TRANSFER FOR SUBCOOLED WATER FLOWING UNDER CONDITIONS OF ZERO GRAVITY

By S. Stephen Papell

Lewis Research Center
Cleveland, Ohio

NATIONAL AERONAUTICS AND SPACE ADMINISTRATION

For sale by the Office of Technical Services, Department of Commerce,
Washington, D.C. 20230 -- Price $0.50

AN INSTABILITY EFFECT ON TWO-PHASE HEAT TRANSFER FOR SUBCOOLED WATER FLOWING UNDER CONDITIONS OF ZERO GRAVITY*

By S. Stephen Papell

Lewis Research Center

SUMMARY

Subcritical, subcooled boiling heat-transfer data were obtained for distilled water flowing through a resistance-heated tube in a gravity-free environment lasting approximately 15 seconds. Two types of flow models were found to exist under identical test conditions. An instability initiated by a momentary interruption of flow forced the transition from a highly subcooled bubbly flow to a postulated slug flow that resulted in a 16-percent increase in local heat-transfer coefficients. The slug-flow regime was described as consisting of two phases in a highly nonequilibrium thermodynamic state. A duplication of test conditions that produced the transition in a zero-gravity environment failed to do so under Earth-gravity conditions.

INTRODUCTION

Forced-flow heat-exchange devices operating in space vehicles can be subjected to flow and heat-transfer phenomena peculiar to a zero- or near-zero-gravity environment. The design of such devices must be based on an understanding of the effect of the gravitational body force on the heat-transfer mechanisms involved. In order to take advantage of the high heat-transfer rates generally associated with forced convective subcooled boiling, an investigation in that particular heat-transfer regime would be warranted. The literature does not contain experimental heat-transfer data for forced convective boiling when the flow system is encountering zero gravity. Described in the literature (refs. 1 and 2) are several zero-gravity pool-boiling experiments that contribute to an understanding of the ebullition process, but the added complexity of the fluid velocity in forced-flow systems minimizes their usefulness.

A general investigation was initiated at the NASA Lewis Research Center to determine the effect of the body force on the heat-transfer mechanism under increased and reduced gravities, including zero gravity. The results reported herein were obtained from a forced-flow water heat-transfer apparatus using a resistance-heated tube for heat flux. The apparatus was installed in the test bed of the NASA airplane zero-gravity facility, where it was possible to provide an environment of approximately 15 seconds of zero and near-zero gravity by flying the airplane through Keplerian trajectories.

---

*Presented at American Rocket Society Meeting, Los Angeles, California, November 13-18, 1962.

Subcritical, subcooled boiling heat-transfer data were obtained throughout the zero-gravity trajectory. The purpose of the experiments given in this report was to determine whether a zero-gravity environment could influence the nature of two-phase flow patterns. Any changes in the flow pattern would be detected in the heat-transfer results. A substantial change in the heat transfer was found after a momentary flow interruption. The change in heat transfer is discussed in terms of an alteration in the flow pattern peculiar to a zero-gravity environment.

SYMBOLS

A	area
c_p	specific heat at constant pressure
d	inside diameter of tube
E	voltage
h	heat-transfer coefficient
I	current
k	thermal conductivity
L	total length of test section
N_{calc}	Nusselt number computed from modified Colburn equation, $0.021\ Re^{0.8}Pr^{0.4}$
N_{exp}	experimental Nusselt number, obtained from measured heat-transfer coefficient, hd/k
Pr	Prandtl number, $c_p\mu/k$
Q	heat flow
q	heat flux per unit area
Re	Reynolds number, $\rho Vd/\mu$
r	radius of tube
T	temperature
V	velocity
x	distance to thermocouple station measured from beginning of heated portion of test section
λ	heat of vaporization

μ viscosity

ρ density

$\dot{\omega}$ mass-flow rate

Subscripts:

av average

b bulk fluid

i inside surface of test section

in inlet

l liquid

o outside surface of test section

s saturation

v vapor

x distance to thermocouple station measured from beginning of heated portion of test section

EXPERIMENTAL EQUIPMENT

Flow System

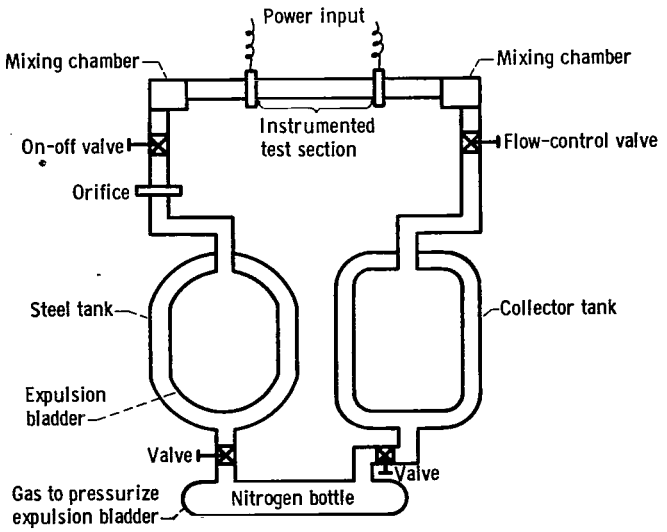

Figure 1. - Schematic drawing of flow system.

Figure 1 is a schematic representation of the flow system for obtaining steady fluid flow through the test section in a zero-gravity environment. Distilled water was contained in a neoprene expulsion bladder installed in the tank upstream of a flow measuring orifice. Nitrogen gas, at controlled pressures, introduced between the inner wall of the tank and the outer surface of the bladder expelled the fluid through the flow system.

Mixing chambers consisting of a system of baffles were installed before and after the test section to eliminate temperature stratification in the fluid bulk. A system of valves and regulators controlled the flow rate and the pressure level

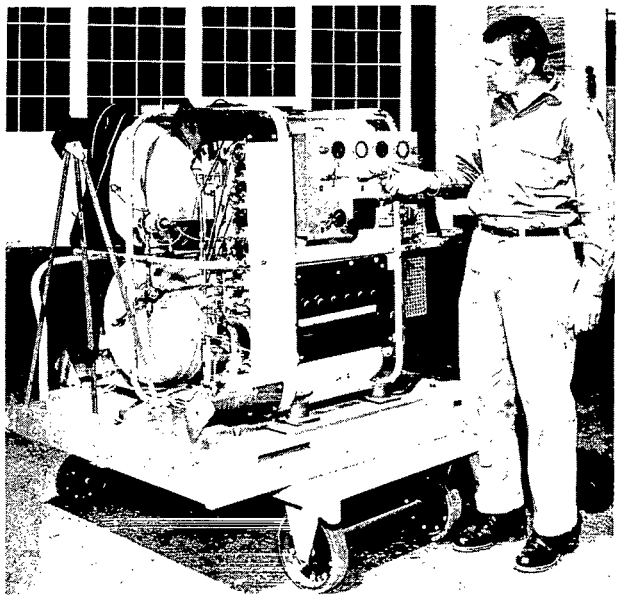

C-61171

Figure 2. - Test apparatus.

throughout the system. The fluid discharged into the collector tank, which also contained an expulsion bladder to allow for recycling. To minimize contamination problems, the piping apparatus was constructed entirely of stainless steel. The apparatus installed in the airplane (fig. 2) was designed to be contained in a 3-foot cube.

Test Section

Figure 3 is a schematic drawing of the instrumented test section showing measuring stations for wall temperatures, pressures, and voltage drops. The nickel-alloy tubing used had a 0.311-inch inside diameter and a 0.012-inch wall thickness. The resistance-heated portion of the test section was 6.5 inches long. Iron-constantan thermocouples, pressure tubes, and voltage taps were silver soldered to the tube.

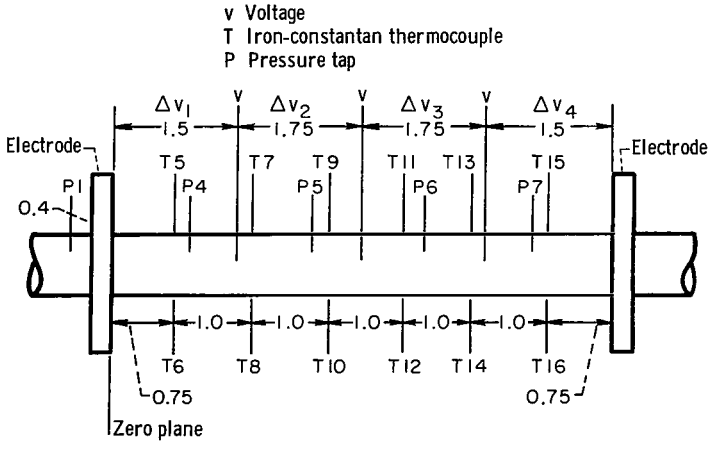

Figure 3. - Schematic drawing of test section showing positions of thermocouples and pressure and voltage taps. (Dimensions in inches.)

A 9000-watt alternator driven by one of the airplane engines supplied power to heat the test section through two electrodes brazed to the outer wall of the tube. The power input was controlled by a system of transformers and a motor-driven powerstat. The vertically installed test section was electrically insulated from the rest of the flow system and was wrapped in fiber glass to minimize ambient heat loss.

Instrumentation

Bulk temperature and pressure measurements were obtained in the mixing chambers located at the inlet and outlet ends of the test section. The test section itself was instrumented with 12 thermocouples made of 28-gage iron-constantan wires installed in two rows along the length of the tube located 180° apart. The five pressure taps were made of 0.035-inch-outside-diameter

stainless-steel thin-wall tubing. The five voltage taps were made of 28-gage copper wires.

All the basic data, including temperatures, pressures, flow rates, and alternating-current tube voltages, were converted to low-voltage direct current so that they could be recorded on a multichannel oscillograph.

Zero-Gravity Facility

The experimental apparatus and the related instrumentation were installed in the test bed of the airplane. The zero-gravity trajectory flown by the airplane consisted of a dive to pick up speed followed by a $2\frac{1}{2}$-g pullup into a ballistic path. Maximum periods of 15 seconds of zero and near-zero gravity were obtained in this manner.

Three accelerometers installed in the test bed directly over the test package measured pitch, yaw, and roll. The frame of the airplane experienced a loading between 0 and 0.02 g throughout the 15-second interval. The test apparatus was tied to the frame of the airplane and was remotely monitored through a control panel installed in the cockpit.

EXPERIMENTAL PROCEDURE

The controlled variables for operating the test apparatus included system pressure, flow rate, and power to heat the test section. With the airplane in position to start the trajectory, the desired system pressure and flow rate were set. At the start of the dive, the electrical power to the test section was turned on to allow time for steady-state conditions to prevail before the zero-gravity portion of the trajectory was entered. The recorders were turned on during the pullup and ran continuously during the balance of the trajectory. After 3 seconds in zero gravity the instability effect reported herein was initiated by a momentary interruption of flow that lasted approximately 1 second. At the end of the trajectory, the power, the flow, and the recorders were turned off, and preparations were made to set up another data run.

The data obtained in this investigation included a system pressure of approximately 50 pounds per square inch absolute, a flow rate of 0.20 pound per second, a heat flux of 1.40 Btu per second per square inch, and a range of subcooling from 175° to 198° F.

Instrumentation calibrations were made prior to each flight by using reference measuring devices to ensure continuous accuracy.

COMPUTATION AND DATA PRESENTATION

Figure 4 is a plot of typical data obtained during the zero-gravity portion of the trajectory and illustrates the change in inside-wall-temperature distribution along the tube before and after the flow perturbation. Inside

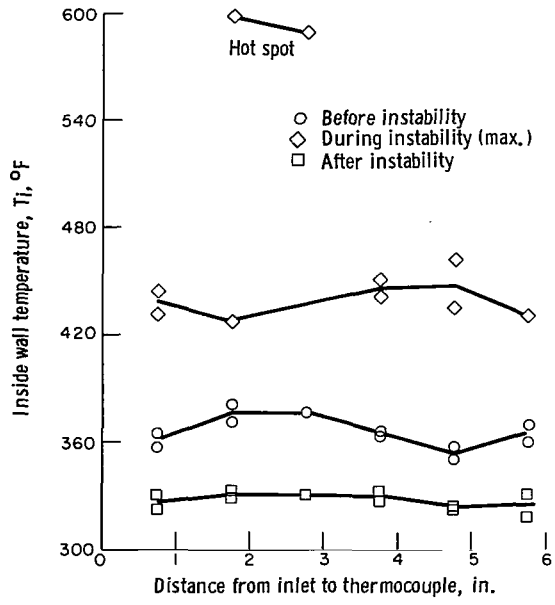

Figure 4. - Changes in wall-temperature distribution along tube before, during, and after flow instability in zero gravity. Steady-state pressure, 44 pounds per square inch absolute; mass flow, 0.19 pound per second; heat flux, 1.40 Btu per second per square inch.

wall temperature is plotted against thermocouple location, and a significant drop in temperature is observed after a flow interruption even though there were only minor changes in test conditions. During the flow interruption the wall temperatures increased approximately 200° F except for several positions that were obviously approaching a dry wall condition or vapor blanketing. A recovery of the flow rate after the short interval of zero flow (1 sec) prevented the tube from burning out. Similar results were obtained during three other trajectories. The difficulty of operating this close to a burnout condition severely limits the amount of data that can be obtained with the present apparatus. Computations were made to determine local values of heat flux, inside wall temperature, and bulk temperature. The heat flux was obtained directly from measured values of current and voltage drop by means of the equation

$$q = 0.948 \times 10^{-3} \frac{EI}{A_i} \qquad (1)$$

The five voltage taps spaced over the length of the test section were used to verify the linearity of the voltage drop to justify using this equation.

Since the heat-transfer coefficient is based on heat flux from the inner surface of the tube, the measured outside wall temperatures were corrected for temperature drop through the wall. A theoretical equation that assumes uniform internal power generation was used (ref. 3):

$$T_i = T_o - \frac{Q\left(r_o^2 \ln \frac{r_o}{r_i} - \frac{r_o^2 - r_i^2}{2}\right)}{k 2\pi L (r_o^2 - r_i^2)} \qquad (2)$$

The local bulk temperatures were obtained by assuming sensible heating of the fluid as indicated by the equation

$$T_{b,x} = T_{b,in} + \frac{Qx}{L\dot{w}c_p} \qquad (3)$$

The second term on the right side of the equation is a measure of the temperature rise of the fluid caused by the heat input. This term was evaluated at each thermocouple station and added to the measured inlet bulk temperature to obtain local bulk temperatures. The sensible heating assumption can be accepted as valid for the data before the instability because of the high sub-

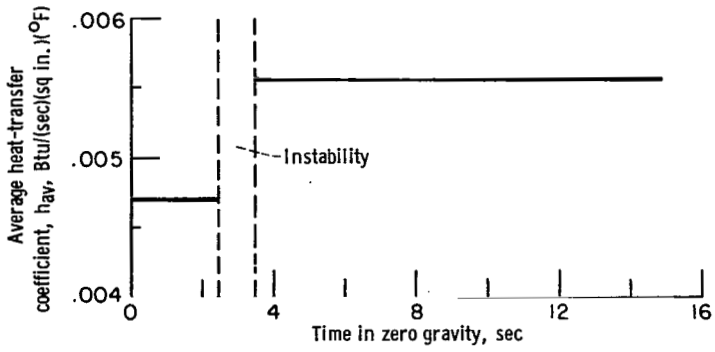

Figure 5. - Change in average heat-transfer coefficients as result of flow instability in zero gravity.

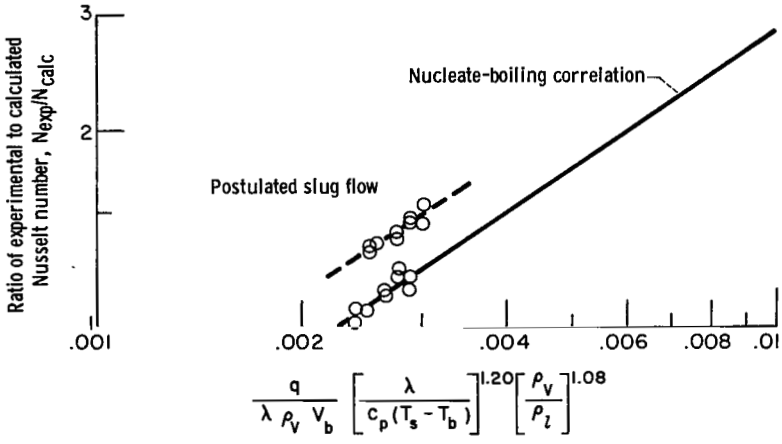

Figure 6. - Comparison between nucleate- and slug-flow data using nucleate-boiling correlating parameter.

cooling involved. It was also used for the data after the instability, even though it is realized that the sensible heating assumption is incorrect, for the fluid described later as consisting of two phases in a highly nonequilibrium state. It is not possible to calculate the amount of latent heat present without knowing the void distribution.

Local heat-transfer coefficients were calculated from the data illustrated in figure 4 by using equations (1), (2), and (3), and the results were averaged on both sides of the instability. Figure 5 is presented to show the change in average heat-transfer coefficient before and after the flow instability. The distance between the vertical dashed lines represents the length of time of wall-temperature fluctuation. The flow perturbation was initiated near the start of the zero-gravity portion of the trajectory, and the change in the average heat-transfer coefficient remained constant throughout the balance of time in zero gravity. The different levels of heat transfer, indicated by the solid lines, represent an increase of the order of 16 percent.

Figure 6 is presented to show that the heat-transfer rates on both sides of the instability are in the boiling regime. The solid line in the figure represents a modified correlation of forced-flow nucleate-boiling heat-transfer data obtained from reference 3. The correlating equation is

$$\frac{N_{exp}}{N_{calc}} = 71.2\left\{\frac{q}{\lambda\rho_v V_b}\left[\frac{\lambda}{c_p(T_s - T_b)}\right]^{1.20}\left(\frac{\rho_v}{\rho_l}\right)^{1.08}\right\}^{0.7} \qquad (4)$$

for values of

$$\frac{q}{\lambda\rho_v V_b}\left[\frac{\lambda}{c_p(T_s - T_b)}\right]^{1.20}\left(\frac{\rho_v}{\rho_l}\right)^{1.08} > 0.00226$$

The parameter plotted on the ordinate is the ratio of the experimentally determined boiling Nusselt number to a calculated nonboiling Nusselt number based on a Colburn-type equation (ref. 4). This ratio remains at a value of unity for all data obtained under nonboiling conditions. When boiling persists, this ratio becomes greater than 1 because of the increased heat-transfer coefficient in the Nusselt number. The incipience of boiling occurs at the point where the Nusselt number ratio departs from a value of unity. The boiling portion of the curve has a slope of 0.7.

The parameter plotted on the abscissa is made up of a group of dimensionless parameters obtained by dimensional analysis from basic considerations. Liquid and vapor densities used in the correlation are evaluated at saturation conditions, and the specific heat is evaluated at the mean temperature between saturation and bulk.

The correlation of reference 5 was applied to the data presented in figure 4 and the results presented in figure 6. Data obtained before the flow instability plot readily along the line representing the nucleate-boiling correlation. Data obtained after the instability plot parallel to the line but consistently high, which indicates a higher heat-transfer coefficient. The percent difference is again of the same order as the change in heat-transfer coefficient plotted in figure 5.

It is significant to note that this increase in heat transfer could be duplicated only under certain test conditions. Many attempts to produce this instability effect resulted in failure when the flow interruption was of insufficient duration to allow the wall temperatures to reach a finite level. Data obtained at higher flow rates also failed to exhibit this trend, even though the flow perturbation was of sufficient magnitude.

DISCUSSION

Boiling-Flow Regimes

At the present time the apparatus used in the experimental investigation cannot be used to obtain a visual indication of any changes that might occur in the flow regime as a result of the flow perturbation. Therefore, explanations are made and conclusions are drawn about the observed changes in heat-transfer rates from the visual studies of two-phase flow discussed in the literature.

It is postulated that the change in heat-transfer rates is due to a transition from highly subcooled nucleate boiling to slug-flow boiling. The nucleate-boiling regime existing before the flow instability is characterized by the formation of bubbles on the heated wall, which depart from the surface while still quite small and condense in the fluid bulk. The heat is transferred away from the wall by means of turbulent mixing as a result of the velocity gradient and the mass transfer caused by bubbles departing from the surface.

The postulated slug-flow regime existing after the instability can be described as containing a mixture of vapor voids, liquid droplets, and Taylor bubbles surrounded by a thin liquid film on the wall. The heat transfer is essentially due to turbulent mixing after conduction through the thin liquid boundary layer. The violent agitation of the fluid is responsible for the increased heat-transfer coefficients obtained in this slug-flow regime.

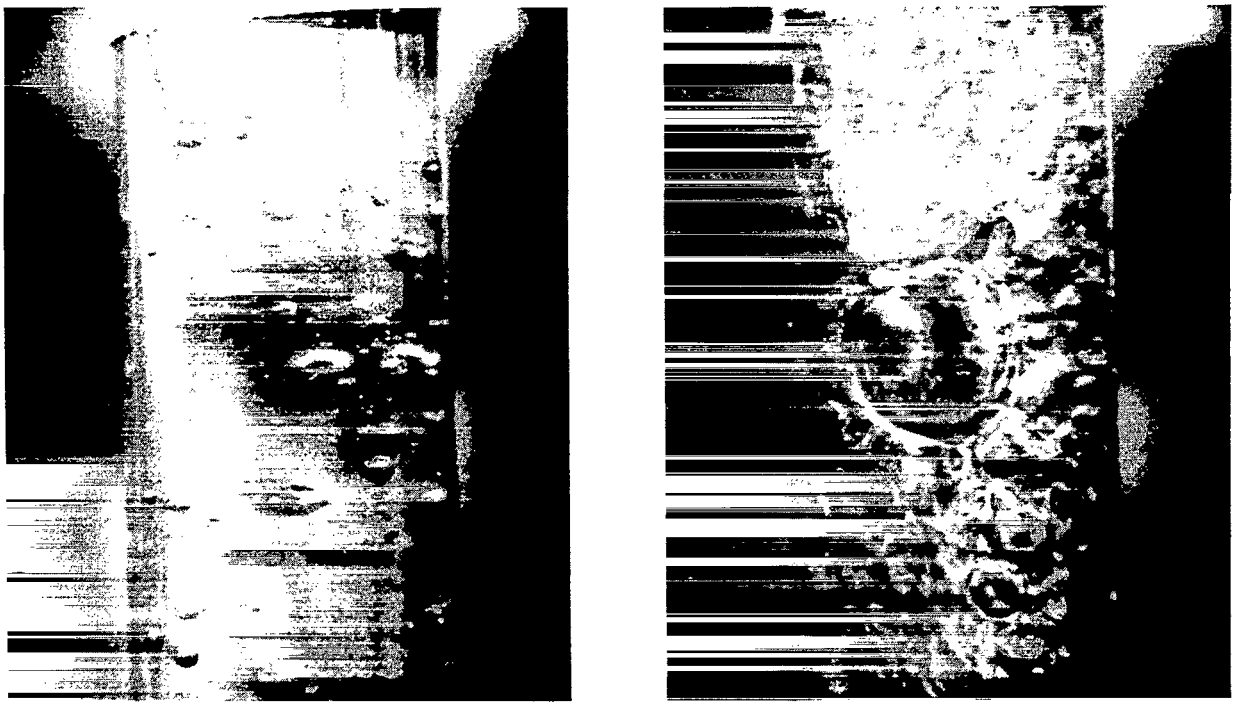

(a) Bubbly flow. (b) Slug flow. C-67455

Figure 7. - Water boiling in vertical, resistance-heated tube under Earth gravity (ref. 5).

Slug Flow Under Earth-Gravity Conditions

Slug flow is reported in referenee 5 for saturated and nearly saturated boiling under Earth-gravity conditions. The two photographs in figure 7 are presented as a visual indication of the types of flow that can exist in subcooled boiling. The prints were obtained from a film supplement to reference 6 showing water boiling in a vertical resistance-heated tube. The transition from bubbly to slug flow in an Earth-gravity environment was effected in this case by increasing the heat input. In both cases the inlet water temperature was 37° below saturation conditions. It is significant to note that the transition took place even though calculations showed that the heat input was insufficient to saturate the fluid. An explanation of this phenomenon, obtained from reference 6, is presented later in this discussion.

Slug Flow Under Zero-Gravity Conditions

The transition from bubbly to slug flow under Earth-gravity conditions, as shown in figure 7, required an increase in quality that was caused by an in-

crease in heat input to the tube. The data obtained in the present investigation indicate that a similar transition took place in a highly subcooled liquid under zero-gravity conditions. The heat input to the tube was held constant during the zero-gravity trajectory, but the increase in quality, in this case, was a result of the rapid increase in wall temperature caused by a momentary flow interruption. It is postulated that, for the period of zero flow, the absence of the buoyancy force contributed to the rapid coalescence of the increased bubble population to force the change in the flow pattern. After the flow rate recovered, the increased heat-transfer coefficients supported the level of quality required to maintain slug flow.

Tests were run with the apparatus under Earth-gravity conditions to establish the need for a zero-gravity environment to allow the flow transition to occur. A duplication of test conditions that produced the transition in zero gravity could not do so in the gravity field. As a result, it is suggested that the presence of the buoyancy force prevents or minimizes bubble coalescence, which is a requirement for the change in the flow pattern.

Degree of Nonequilibrium

The existence of two distinct flow regimes under identical test conditions in a zero-gravity environment can be explained in terms of thermodynamic equilibrium. In reference 6 the experimental data that were presented showed the existence of a highly nonequilibrium boiling two-phase flow system. Photographic evidence presented in reference 6 showed that considerable volumes of vapor could coexist with subcooled liquid. To explain this phenomenon, a heat balance in and out of a cross-sectional control volume in the boiling fluid was considered. The amount of vapor that can exist in a subcooled flow is based on the net result of the rate of evaporation at the wall plus the vapor entering the volume minus the rate of condensation in the stream. The results showed that, the more heat expended for evaporation, the less available as sensible heat and the farther the system from thermal equilibrium. The degree of nonequilibrium therefore depends on the difference between the rates of evaporation and condensation. Controlling parameters for these two heat-transfer processes are numerous. The rate of evaporation is a function of heat flux, surface conditions, subcooling, and flow rate. The rate of condensation depends on the initial bubble velocity, the turbulence of the flow, and the amount of subcooling.

It is postulated that a similar highly nonequilibrium state exists in the zero-gravity flow regime described in this report. During the flow instability, the zero-flow condition increased the bubble population, which coalesced into large voids. This reduction in the liquid vapor interface and the lack of turbulence resulted in a decreased condensation rate. The result was a highly nonequilibrium two-phase regime, which persisted even after the flow rate recovered. The drop in wall temperature recorded at this time was a direct result of more heat being expended for evaporation than before the instability. Photographic studies would be an invaluable aid in attempting to determine the rates of evaporation and condensation that could exist under different test conditions.

CONCLUDING REMARKS

The results of the present investigation show that two distinct types of subcooled boiling flow can exist under identical test conditions in a gravity-free environment. Since both types of flow persist, a perturbation is required to force the transition from one to the other. In this case, the instability was initiated by a momentary flow interruption. The postulated change from a highly subcooled bubbly flow to a slug flow resulted in increases in heat-transfer coefficient of the order of 16 percent. The bubbly-flow regime was considered to be close to thermal equilibrium, but the slug-flow regime was described as existing in a highly nonequilibrium state. The difference in heat-transfer coefficient in both flow regimes can be used as a measure of the degree of nonequilibrium that exists.

Further studies are being made to attempt to map out the conditions that must exist to cause the transition to occur. It has been established that the magnitude of the perturbation and the initial velocity of the fluid are significant parameters. Experimental data show that, when the perturbation is too small and/or the velocity is too high, the transition does not take place. A duplication of test conditions that produced the transition in a zero-gravity environment failed to do so under Earth-gravity conditions. Any attempt to make use of the heat-transfer phenomenon described in this paper must be preceded by much more investigation.

Lewis Research Center
National Aeronautics and Space Administration
Cleveland, Ohio, January 2, 1964

REFERENCES

1. Siegel, R., and Usiskin, C. M.: A Photographic Study of Boiling in the Absence of Gravity. ASME Trans. Heat Trans., Series C, vol. 81, 1959, pp. 230-236.

2. Usiskin, C. M., and Siegel, R.: An Experimental Study of Boiling in Reduced and Zero Gravity Fields. ASME Trans. Heat Trans., Series C, vol. 83, 1961, pp. 243-253.

3. Papell, S. Stephen: Subcooled Boiling Heat Transfer Under Forced Convection in a Heated Tube. NASA TN D-1583, 1963.

4. McAdams, W. H.: Heat Transmission. McGraw-Hill Book Co., Inc., 1954, pp. 19 and 219.

5. Sachs, P., and Long, R. A. K.: A Correlation for Heat Transfer in Stratified Two-Phase Flow with Vaporization. Int. J. Heat Mass Trans., vol. 2, 1961, pp. 222-230.

6. Hsu, Yih Y., and Graham, Robert W.: A Visual Study of Two-Phase Flow in a Vertical Tube with Heat Addition. NASA TN D-1564, 1963.

NASA-Langley, 1964 E-1833

2/17/85

"The aeronautical and space activities of the United States shall be conducted so as to contribute . . . to the expansion of human knowledge of phenomena in the atmosphere and space. The Administration shall provide for the widest practicable and appropriate dissemination of information concerning its activities and the results thereof."

—NATIONAL AERONAUTICS AND SPACE ACT OF 1958

NASA SCIENTIFIC AND TECHNICAL PUBLICATIONS

TECHNICAL REPORTS: Scientific and technical information considered important, complete, and a lasting contribution to existing knowledge.

TECHNICAL NOTES: Information less broad in scope but nevertheless of importance as a contribution to existing knowledge.

TECHNICAL MEMORANDUMS: Information receiving limited distribution because of preliminary data, security classification, or other reasons.

CONTRACTOR REPORTS: Technical information generated in connection with a NASA contract or grant and released under NASA auspices.

TECHNICAL TRANSLATIONS: Information published in a foreign language considered to merit NASA distribution in English.

TECHNICAL REPRINTS: Information derived from NASA activities and initially published in the form of journal articles.

SPECIAL PUBLICATIONS: Information derived from or of value to NASA activities but not necessarily reporting the results of individual NASA-programmed scientific efforts. Publications include conference proceedings, monographs, data compilations, handbooks, sourcebooks, and special bibliographies.

Details on the availability of these publications may be obtained from:

SCIENTIFIC AND TECHNICAL INFORMATION DIVISION

NATIONAL AERONAUTICS AND SPACE ADMINISTRATION

Washington, D.C. 20546